A Simplified Model for the Rolling Shutter Based Camera in Optical Camera Communications

Xicong Li*, Navid Bani Hassan*, Andrew Burton*, Zabih Ghassemlooy*,
Stanislav Zvanovec†, Rafael Perez-Jimenez‡
*Optical Communications Research Group, Northumbria University, Newcastle upon Tyne, UK
†Czech Technical University in Prague, Prague, Czech Republic
‡IDeTIC, University of Las Palmas de Gran Canaria, Las Palmas de Gran Canaria, Spain
*{xicong.li, navid.hassan, andrew2.burton, z.ghassemlooy}@northubria.ac.uk,
†xzvanove@fel.cvut.cz, ‡rafael.perez@ulpgc.es

***Abstract*—A simplified model of the camera for optical camera communications (OCC) based on the rolling shutter effect is proposed and experimentally verified. In OCC, the key parameters are the exposure time, which is proportional to the DC gain and inversely proportional to the bandwidth, and the rolling shutter delay or the sampling period. We demonstrate a good agreement between experimental and numerically simulated results for the proposed receiver model.**

***Index Terms*—Visible light communications, optical camera communications, rolling shutter, camera communication, image sensor, frequency response**

I. Introduction

Visible light communications (VLC) have emerged as a promising technology in wireless communication and attracted substantial research interests due to advantages such as the multiple functionality of illumination, communication, indoor localisation, unlicensed spectrum, no electromagnetic interference and inherent security [1]. Optical camera communications (OCC) operate in the same band as VLC but use built-in cameras in smart devices as receivers, thus providing more system flexibility and lower cost.

The core of a camera in smart devices is a complementary metal-oxide-semiconductor (CMOS) image sensor. Generally, the image sensor can operate in global shutter mode or rolling shutter mode. In global shutter mode, all pixels are exposed to light simultaneously to form one frame and only when each pixel in the old frame is read out a new frame can be captured. In other words, the frame rate is dominating the maximum data rate for OCC systems using global shutter cameras. Typically smartphone cameras can run at a relatively low frame rate such as 30 fps (frame per second) [2], whereas specific cameras may reach 1000 fps [3] or higher.

The rolling shutter cameras successively expose pixels in each horizontal line and read out the exposed line at the same time to speed up the operating data rate. The rolling shutter mechanism enables the camera to detect the change of light intensity over rows in one frame, while the global shutter cameras have to capture consecutive frames. Although the rolling shutter mode will result in unwanted artefacts when taking photos in motion, it offers a higher data rate and therefore is preferred in OCC [1], [4].

In addition, the exposure and pixel array of cameras makes the characteristics of OCC systems different from conventional VLC systems based on photodiodes and transimpedance amplifier (TIA) circuits. As discussed later, the exposure time plays a vital role on the system bandwidth as well as the gain; the array of pixels introduces space distortion or space modulation when an actual light source with a geometric shape is used. If multiple sources are employed, the OCC system can benefit from this inherent architecture for multiple-input-multiple-output (MIMO) [5] systems.

In this paper, we focus on the modelling of the rolling shutter based camera using CMOS image sensors and analyse the key parameters and their effects on the OCC system. Using an experimental testbed, we verify the predicted frequency response and show that there is a good match between them.

The rest of the paper is organised as follows. Section II briefly introduces the OCC system architecture with a CMOS image sensor and proposes a model taking optical and electrical effects into account. In Section III, the frequency response for different exposure time are measured, and experiment results are provided. Section IV concludes the paper.

II. Camera Model

As shown in Fig. 1, the simplified camera model can be divided into three parts: (*i*) the optics for imaging formation; (*ii*) the exposure; and (*iii*) the conversion from a continuous signal to a discrete time signal using an ADC.

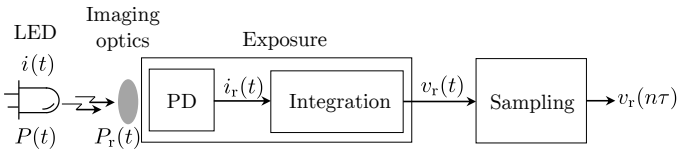

Fig. 1. The Simplified model for cameras in OCC

At the transmitter, $i(t)$ is the modulation current driving the light-emitting diode (LED), and the corresponding optical power $P(t)$ is assumed to be proportional to $i(t)$ as for simplicity we do not consider the nonlinearity of the LED here. At the camera, $P_{\mathrm{r}}(t)$ is the received optical power at

one pixel[1] and then converted to current by a photodiode (PD) inside the pixel. After integration during the exposure time T, certain amount of charges will accumulate and the voltage signal across the equivalent photodiode capacitance C_{PD} , which is equal to $\frac{1}{C_{\mathrm{PD}}}\int_{t-T}^{t} i_{\mathrm{r}}(t)\,\mathrm{d}t$, is then amplified by a factor of g and sampled by the ADC and read out with a period of τ [6].

For illustrative purposes, Fig. 2 shows a line-of-sight (LOS) based OCC system including a light source, for instance, a LED with a Lambertian emission pattern [7], a lens as a representative of camera imaging optics, and a CMOS image sensor. Because of the imaging mechanism and the size of the light source, the light source will occupy a certain area in the camera's image plane, making one pixel differ in the received optical power from other pixels even when the illuminance of light source keeps constant. In the camera's image sensor, pixels in one horizontal line are exposed to light at the same time, and each row gets exposed in sequence. After exposure, each row is then sampled and read out successively.

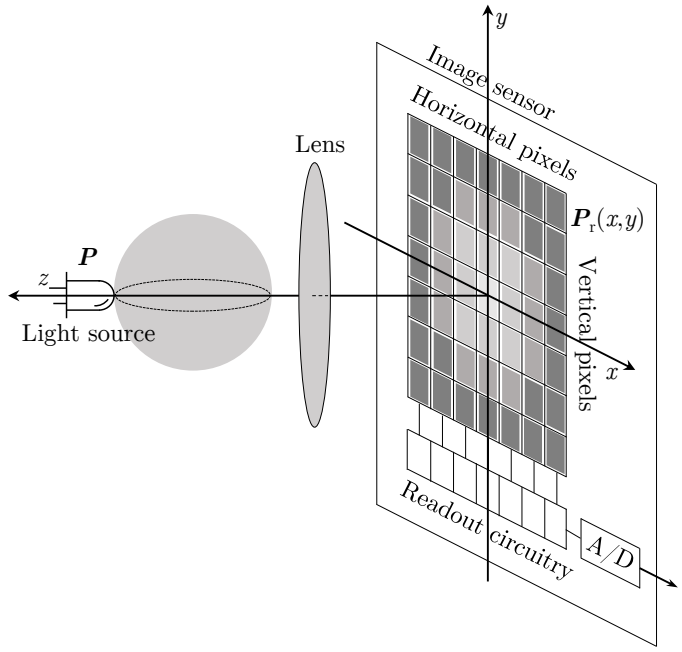

Fig. 2. Camera communication diagram

A. Imaging Optics

As mentioned previously, due to the imaging optics of the camera, the array of pixels in the image sensor can detect modulated light intensity at different positions. To avoid the complexity of modelling the camera lenses system [8], an optical power distribution function $I(x, y)$ in the camera's imaging plane is defined as [9]

$$I(x,y) = \frac{P_{\mathrm{r}}(x,y,t)}{P(t)} \tag{1}$$

[1]The received power also depends on the position of the pixel.

where (x, y) donotes the pixel in the camera coordinate system, and $P_{\mathrm{r}}(x, y, t)$ is the received optical power by the pixel (x, y) at the time constant t.

The distribution function $I(x, y)$ is introduced to account for the waveform distortion introduced in space due to the power distribution variance at different pixels. To make the notation clear, x and y are omitted in other signals because the space modulation only takes effect in the imaging optics part. Here the LOS VLC channel is assumpted with an ideal channel with infinite bandwidth based on the fact that the bandwidth of a LOS VLC channel [10] is much higher than the bandwidth of a camera.

Then the current flown through the photodiode in the pixel (x, y) can be calculated by

$$i_{\mathrm{r}}(t) = RP_{\mathrm{r}}(t) \tag{2}$$

where R is the responsivity of the photodiode in the pixel.

B. Exposure (Integration)

The voltage across the photodiode after exposure is given by [6]

$$v_{\mathrm{r}}(t) = \frac{g}{C_{\mathrm{PD}}}\int_{t-T}^{t} i_{\mathrm{r}}(t)\,\mathrm{d}t \tag{3}$$

where g is the amplifier gain. Hence the corresponding impulse response is

$$h(t) = \frac{g}{C_{\mathrm{PD}}}\big(u(t) - u(t-T)\big) \tag{4}$$

where $u(t)$ is the unit step function.

The frequency response is given by

$$H(f) = \mathscr{F}\{h(t)\} = \frac{gT}{C_{\mathrm{PD}}}\frac{\sin(\pi fT)}{\pi fT}\mathrm{e}^{-j\pi fT} \tag{5}$$

where $j = \sqrt{-1}$, f is the frequency, and $\mathscr{F}$ denotes the Fourier transform operation.

1) 2-dB bandwidth and the roll-off rate: As $|H(f)|$ has a series of zeros given by $f_z = \frac{n}{T}$, $n = 1, 2, \cdots$, $|H(f)|$ shows steep notches at these points. Additionally, $|H(f)| \leq \frac{gT}{C_{\mathrm{PD}}} \cdot \frac{1}{\pi fT}$ and the equality holds for peaks between zeros $f_p = \frac{n}{T} + \frac{1}{2T}$, hence the local peaks of $|H(f)|$ between the zeros roll off at $-20\,\mathrm{dB/dec}$. [2] Note that a loss of $-2\,\mathrm{dB}$ (i.e. $20\log\frac{2}{\pi}$) is introduced at the first peak $f_p = \frac{1}{2T}$.

2) DC gain: The DC gain can be interpreted as a scaling factor by which the amplitude is attenuated or amplified, therefore having a significant effect on the maximum achievable signal-to-noise ratio (SNR). Theoretically the DC gain can be computed by

$$|H(0)| = \lim_{f\to 0}|H(f)| = \frac{gT}{C_{\mathrm{PD}}} \tag{6}$$

or

[2]Since $20\log\frac{1}{f} = -20\log f$, $-20\,\mathrm{dB/dec}$ can be observed if using the logarithmic scale.

$$|H(0)| = \int_{-\infty}^{+\infty} h(t)\,\mathrm{d}t = \frac{gT}{C_{\mathrm{PD}}} \tag{7}$$

This agrees with our intuition that the larger gain comes with more optical power collected during a longer exposure time. Fig. 3 illustrates the process in the electrical domain with four horizontal lines successively exposed to light modulated with DC biased sine wave. The exposure introduces an amplification of factor $\frac{gt}{C_{\mathrm{PD}}}$ between the DC values of $i_{\mathrm{r}}(t)$ and $v_{\mathrm{r}}(t)$. Due to the non-negativity of optical signal, the peak-to-peak amplitude of $v_{\mathrm{r}}(t)$ cannot be greater than $\frac{2gAT}{C_{\mathrm{PD}}}$, where A is the DC offset of $i_{\mathrm{r}}(t)$.

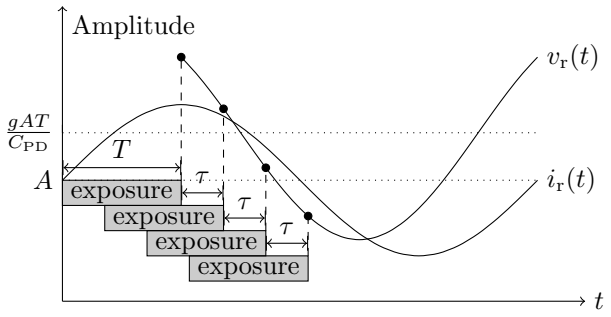

Fig. 3. Illustrative diagram of 4 horizontal lines successively exposed in rolling shutter mode

C. Sampling

The third part of the model is the sampling process to convert the continuous-time signal $v_{\mathrm{r}}(t)$ after integration into the discrete-time signal $v_{\mathrm{r}}(n\tau)$ with a sampling period of τ:

$$v_{\mathrm{r}}(n\tau) = v_{\mathrm{r}}(t) \sum_{n} \delta(t - n\tau) \tag{8}$$

where $\delta(t)$ is the Dirac delta function, and τ is the sampling period.

From the Nyquist sampling theorem only signals with bandwidth $B < \frac{1}{2\tau}$ can be reconstructed correctly without aliasing. The question of what determines τ then arises.

For a CMOS image sensor in rolling shutter mode (Fig. 2), the sampling period τ defined in Fig. 3 is essentially the pipeline process delay of the ADC to handle one horizontal line of pixels, which is approximately given by

$$\tau = \frac{\text{Horizontal Width} \times \text{ADC Resolution Per Pixel}}{\text{ADC Sampling Data Rate}} \tag{9}$$

This is because the ADC is time-multiplexed and only after the last line has been processed the newly exposed line can be sampled. For example, in the case of the image sensor MT9P001 [11], τ can be estimated by $\frac{2592\,\text{pixel}}{96\,\text{Mpixel/s}} \approx 27\,\mu\text{s}$, which agrees well with the parameter in the datasheet. [3] It can also be concluded from (9) that the rolling shutter delay or readout delay can be reduced if the horizontal width is decreased, thus enabling increased equivalent sampling rate in one rolling shutter frame and higher bandwidth. This is one benefit of the feature of the region of interest (ROI) [12] but at the cost of data loss in one frame.

To sum up, the optics part describes the optical power distribution function determined by the camera's imaging system, which is dependent on the geometric relationship between the light source and the camera. The exposure is equivalent to integration over a period of time and decides the system bandwidth in the continuous time domain. Finally, the sampling process determines the maximum system bandwidth following the Nyquist sampling theorem.

III. Measurement Setup and Results

A. Measurement Setup and Procedure

The experimental setup is shown in Fig. 4 and the procedure is as follows:

1) drive the red LED (Cree C503B-RAN-CA0B0AA1) by DC biased sine wave directly from a function generator (Agilent 33220A);
2) align the smartphone (Huawei Honor STF-AL00, camera resolution 3968×2976, 10 bit) with the LED with a diffuser placed between them to capture a large area of the light source by the camera;
3) fix the exposure time and all other parameters of the camera;
4) sweep the frequency and capture 100 pictures in the raw file format at each frequency;
5) change the exposure time only and repeat step (3) and (4);
6) compute the average peak-to-peak value from captured raw pictures and plot the frequency response for this specific exposure time.

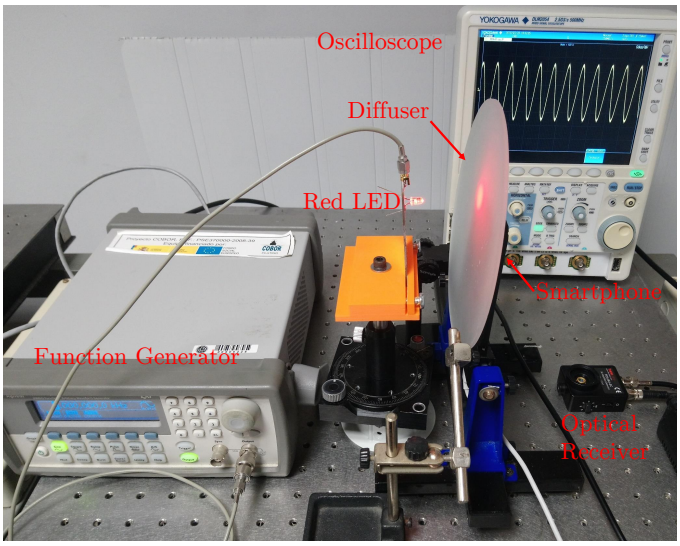

Fig. 4. Experimental setup

The function generator was set in continuous sine wave mode with a peak-to-peak voltage of 600 mV and an offset

[3] Here the parameter refers to t_{ROW} in the datasheet

of 1.25 V.[4] Pictures were captured in a dark room using OpenCamera with an ISO of 50 and focused at infinity. Before carrying on the experiment, an optical receiver (Thorlab PDA36A, 10 dB gain, 5.5 MHz) together with an oscilloscope (Yokogawa DLM2054, 2.5 GSa/s, 500 MHz) was used to check if the LED was modulated correctly. A modulation depth of around 84% was achieved.

B. Optical Power Distribution $I(x, y)$ and Compensation

Fig. 5 shows the intensity distribution on the camera image plane when biasing the LED with DC offset only. Since a DC signal was applied, the measured intensity distribution is then proportional to the optical power distribution function $I(x, y)$ from (1). This distribution function is only dependent on the geometry and stays the same if the setup is fixed. Fig. 6 illustrates the intensity detected at different pixels for the 200 Hz sine wave. As dicussed in Section II, Fig. 6 can be interpreted as a sine wave modulated by the DC intensity distribution $I(x, y)$ in Fig. 5.

Because pixels in each horizontal line are exposed to light at the same time, they only suffer from the DC intensity distortion from the geometry and do not contribute to the rolling shutter effect. So only the vertical line which passes through the intensity peak was selected to calculate the received signal strength for the frequency response. The dimensionality reduction from this operation leads to

$$I(x, y)|_{x=x_0} = I(x_0, y) = I(y) \tag{10}$$

Here we choose the following polynomial function to fit with the DC intensity profile

$$\hat{I}(y) = G\big((y - C)^2 + D^2\big)^{-2} \tag{11}$$

where G, C and D are coefficients to be fitted. C is introduced to account for the axis of symetry in image processing. With the intensity distribution function, we can apply compensation or equalisation to the received signal intensity $I_{\text{pixel}}(y)$ at pixel (x_0, y) by multiplying $\frac{1}{\hat{I}(y)}$.

The measured DC intensity profile for the 1974^{th} line and fitted curve with (10) are shown in Fig. 7. [5] The amplitude of the sine wave becomes flat after compensation, which enables the measurement of the received signal amplitude. To avoid noise amplification at the beginning and end of the row of pixels where the DC intensity attenuates the most, which is similar to the zero forcing equaliser, only pixels $\in [700, 800]$ have been selected.

The sampling period τ can be approximately estimated by $\frac{5\,\text{ms}}{1500/6.5} \approx 22\,\mu\text{s}$, [6] and then the Nyquist frequency $\frac{1}{2\tau} \approx 23\,\text{kHz}$ is determined correspondingly. The experiments were conducted below the Nyquist frequency to avoid aliasing. It is also worth mentioning that because of the limited ADC resolution of the camera the distance between the LED and the smartphone was reduced to increase DC gain for shorter exposure time.

[4]The 1.25 V offset can turn the LED on because the function generator displays the voltage as if it was terminated into a 50 Ω load. The equivalent voltage source inside is twice the display voltage.

[5]The number of vertical pixels in Fig. 7 is reduced by half because only pixels in the red channel are used to eliminate the Bayer filter effect. This also explains why raw file format was adopted in this experiment.

[6]In Fig. 7 about 6.5 cycles of the 200 Hz are found in 1500 vertical pixels. So there are $1500/6.5$ samples in every 50 ms. Note that here 22 µs accounts for delays between every other line (red channel). The real rolling shutter delay is half of the value.

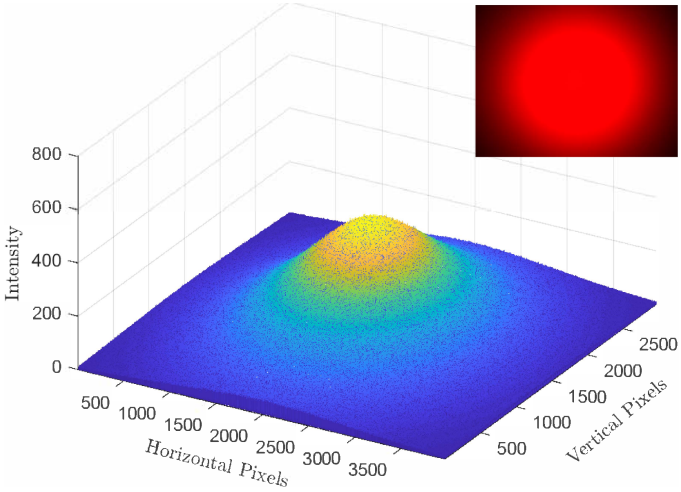

Fig. 5. DC intensity distribution on the camera image plane

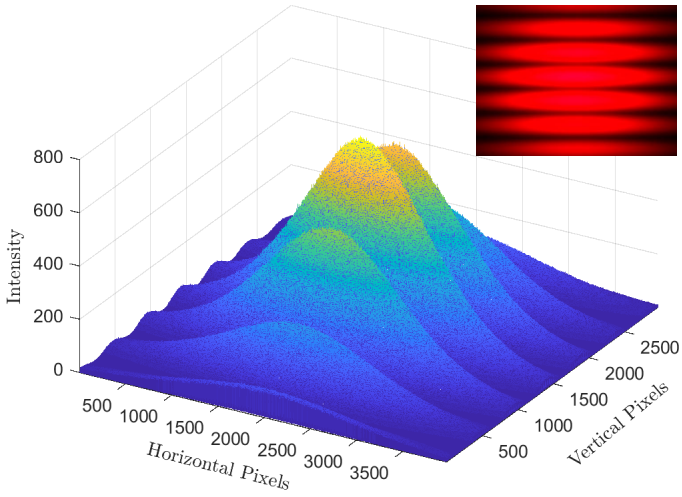

Fig. 6. Received 200 Hz sine wave on the camera image plane

Fig. 7 plots measured and theoretical frequency response for $T = 1\,\text{ms}$ and $T = 0.1\,\text{ms}$ as well as the reference line $\frac{1}{\pi f T}$ with a slope rate of $-20\,\text{dB/dec}$. The response for $T = 1\,\text{ms}$ are normalized to 0 dB while those for $T = 0.1\,\text{ms}$ normalized to $20 \log \frac{0.1\,\text{ms}}{1\,\text{ms}} = -20\,\text{dB}$. It can be observed that the measured curves are consistent with the proposed model up to the Nyquist frequency.

IV. Conclusion

The simplified model for rolling shutter based cameras had been proposed and verified experimentally. The model and measurement results agreed well and provided insights on how to evaluate the performance of an OCC system.

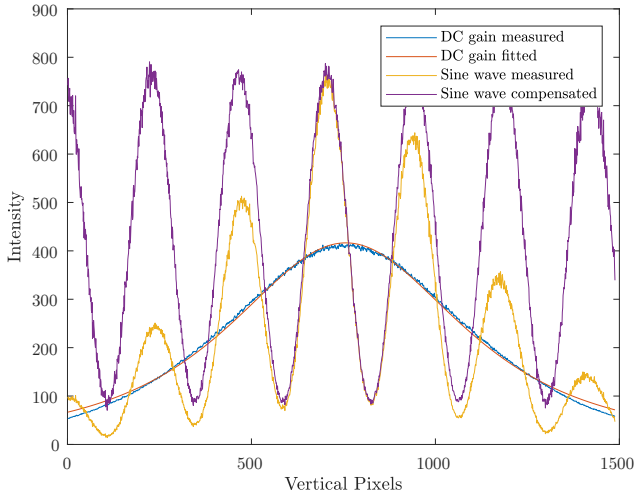

Fig. 7. Compensation of the 200 Hz sine wave using DC intensity distribution (the 1974$^{\text{th}}$ vertical line in Fig. 5 and Fig. 6)

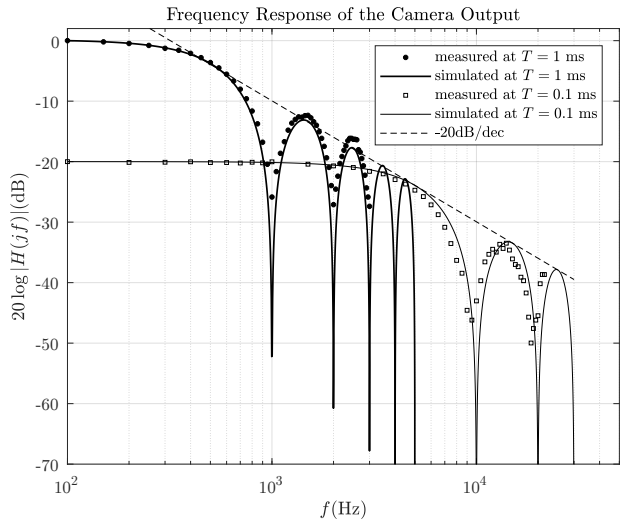

Fig. 8. The frequency response for exposure time $T = 1$ ms and $T = 0.1$ ms

It was evidenced that the gain bandwidth product is the principle governing the exposure channel. In other words, higher bandwidth is achieved at the cost of lower gain. As to the sampling, the Nyquist frequency is determined by the working mechanism of the image sensor and related with the image sensor's processing latency. A tradeoff must be made between bandwidth, gain, sampling rate and net data rate per frame.

V. Acknowledgment

This work is supported by the European Union's Horizon 2020 research and innovation programme under the Marie Sklodowska-Curie grant agreement n$^{\text{o}}$ 764461 (VISION), the UK EPSRC research grant EP/P006280/1: MARVEL and the Czech Science Foundation project GACR 17-17538S.

References

[1] Z. Ghassemlooy, L. N. Alves, S. Zvanovec, and M.-A. Khalighi, *Visible Light Communications: Theory and Applications*. CRC Press, 2017.

[2] P. Luo, Z. Ghassemlooy, H. L. Minh, X. Tang, and H. M. Tsai, "Undersampled phase shift on-off keying for camera communication," in *2014 Sixth International Conference on Wireless Communications and Signal Processing (WCSP)*, 2014, Conference Proceedings, pp. 1–6.

[3] Sony, "Dsc-rx10m2."

[4] T. Nguyen, A. Islam, T. Yamazato, and Y. M. Jang, "Technical issues on ieee 802.15.7m image sensor communication standardization," *IEEE Communications Magazine*, vol. 56, no. 2, pp. 213–218, 2018.

[5] N. Bani Hassan, Z. Ghassemlooy, S. Zvanovec, M. Biagi, A. M. Vegni, M. Zhang, and P. Luo, "Non-line-of-sight mimo space-time division multiplexing visible light optical camera communications," *Journal of Lightwave Technology*, pp. 1–1, 2019.

[6] J. C. Chau and T. D. C. Little, "Analysis of cmos active pixel sensors as linear shift-invariant receivers," in *2015 IEEE International Conference on Communication Workshop (ICCW)*, 2015, Conference Proceedings, pp. 1398–1403.

[7] Z. Ghassemlooy, W. Popoola, and S. Rajbhandari, *Optical wireless communications: System and Channel Modelling with MATLAB*. CRC Press, 2012.

[8] R. D. Fiete and B. D. Paul, *Modeling the optical transfer function in the imaging chain*. SPIE, 2014, vol. 53.

[9] M. S. Ifthekhar, M. A. Hossain, C. H. Hong, and Y. M. Jang, "Radiometric and geometric camera model for optical camera communications," in *2015 Seventh International Conference on Ubiquitous and Future Networks*, July 2015, pp. 53–57.

[10] T. Komine and M. Nakagawa, "Fundamental analysis for visible-light communication system using led lights," *IEEE Transactions on Consumer Electronics*, vol. 50, no. 1, pp. 100–107, 2004.

[11] "Mt9p001 1/2.5-inch 5 mp cmos digital image sensor," 2017.

[12] S. Vitek, J. Libich, P. Luo, S. Zvanovec, Z. Ghassemlooy, and N. Bani Hassan, "Influence of camera setting on vehicle-to-vehicle vlc employing undersampled phase shift on-off keying," *Radioengineering*, vol. 26, pp. 949–953, 12 2017.